Fatigue behaviour of infrared welded joints in fibre reinforced thermoplastics

Ives De Baere, Klaas Allaer, Wim Van Paepegem and Joris Degrieck
Department of Materials Science and Engineering, Ghent University, Technologiepark-Zwijnaarde 903, B-9052 Zwijnaarde, Belgium

ABSTRACT

Due to the increasing interest in fibre reinforced thermoplastics, there is also a need for a reliable means of bonding them. As thermoplastics have a high chemical inertness, adhesive bonding is not always an option and thus, fusion bonding might prove an interesting solution. This manuscript presents an infrared welding process for a carbon fabric reinforced polyphenylene sulphide. A one sided and a two sided welding process is described and the welding parameters are optimised by performing quasi-static lapshear tests for different welding parameters. As the two sided welding process yields the most promising results with respect to reproducibility and strength, two sided welded specimens are also tested under fatigue loading conditions. Here, the applied maximum load has a large influence on the fatigue life and when lower load levels are considered, significant crack growth occurs before final failure.

1. INTRODUCTION

As the industry starts to see the growing potential of fibre reinforced thermoplastics, it is more likely to choose this group of reinforced plastics over the fibre reinforced thermosetting polymers. However, where thermosetting polymers are in general easily bonded using adhesives, this is not always the case for thermoplastics, given their chemical inertness.
As load bearing joints cannot always be avoided, there is a growing interest welding processes for thermoplastic composites and although fusion bonding of pure thermoplastics is already a well known and commonly applied production process, the process parameters cannot be extrapolated to the welding of fibre-reinforced thermoplastics, since the reinforcement has a large influence as the material is no longer isotropic in mechanical properties, nor in thermal properties.
In general, these fusion bonding techniques can be categorised in three groups [1]: (i) frictional welding, including ultrasonic welding [2, 3]; (ii) electromagnetic welding, including resistance welding [4, 5] and induction welding [6, 7] and (iii) thermal welding, including infrared welding [8].

To assess the strength and reproducibility of the weld, quasi-static experiments till failure are quite often considered. Until now, there is not yet a standardised method for testing welded joints, but there are various standards and test setups available for examining the strength of adhesive bonds or the growth of delaminations [9, 10]. These include (a) the Double Cantilever Beam test (DCB) which induces pure Mode I crack-growth, (b) the End Notch Flexure beam test (ENF), both three- point and four-point, which imposes pure Mode II crack-growth, (c) the Mixed Mode Bending (MMB) experiment which combines combined Mode I and II at a given ratio and (d) the Lap Shear Strength test (LSS), a structural test with also a combination of Mode I and Mode II. For evaluating the strength and the quality of the welds, the most commonly chosen experimental setups are the LSS [3, 4] and DCB [8]. These methods give relevant information about the quality of the weld and are also quite useful for comparative studies [5].

In this manuscript, the infrared welding process is considered to bond a 5-harness satin weave carbon reinforced polyphenylene sulphide (PPS). The quality of the bonds is assessed using lapshear experiments, as this is the most commonly used test to evaluate the bond. In the next paragraph, both the composite material and the welding apparatus are discussed in detail. Then, the welding process itself is discussed after which the lapshear experiments, both quasi-static and fatigue, are illustrated. Finally, some conclusions are drawn.

2. MATERIALS AND METHODS

2.1. Composite Material

The material under study is a carbon fabric reinforced polyphenylene sulphide (PPS) composite, called CETEX®, which was supplied by the company Ten Cate. The fibre type used is the carbon fibre T300J 3K and the weave pattern is a 5-harness satin weave, one stacking sequence was used for this study, namely $[(0^o, 90^o)]_{4s}$ where $(0^o, 90^o)$ represents one layer of fabric. The plates were produced by hot pressing at a temperature of 310

°C and a pressure of 10 bar. The in-plane elastic properties and the tensile strength properties of the CETEX® composite are listed in in Table 1.

Table 1 – In-plane elastic and tensile strength properties of the individual carbon/PPS lamina

E_{11} [GPa]	E_{22} [GPa]	ν_{12} [-]	G_{12} [GPa]	X_T [MPa]	ε_{11}^{ult} [-]	Y_T [MPa]	ε_{22}^{ult} [-]	S_T [MPa]
56.0	57.0	0.033	4.175	736	0.011	754.0	0.013	110.0

The test coupons were sawn with a water-cooled diamond saw. Figure 1 shows the geometry of both a fusion bonded batch with adhesively bonded tabs (top) and the single lapshear specimen (bottom), which is cut from it. The width of a welded badge is always so that three lapshear specimens could be cut. The X symbolises the welding cycle and the specimens are numbered consecutively (LS-X-01 to LS-X-03). The dimensions are chosen according to the ASTM D5868-01 '*Standard Test Method for Lap Shear Adhesion for Fiber Reinforced Plastic Bonding*'.

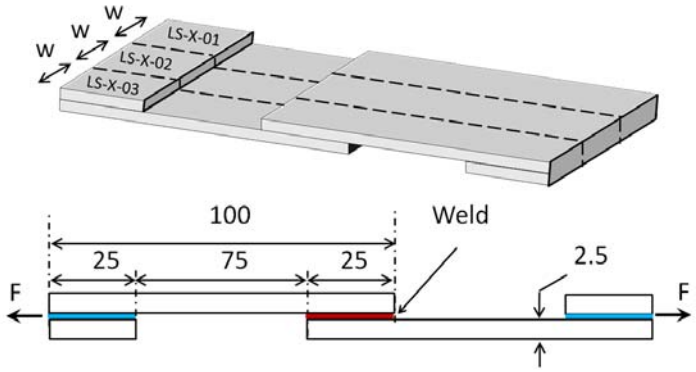

Figure 1 – Dimensions of the used single lapshear specimen (in mm)

2.2. Equipment

All tensile tests were performed on an servo-hydraulic INSTRON 8801 tensile testing machine with a FastTrack 8800 digital controller and a load cell of ±100kN. The quasi-static tests were displacement-controlled with a displacement speed of 1 mm/min. For the registration of the tensile data, a combination of a National Instruments USB 6251 data acquisition card and the SCB-68 pin shielded connecter were used. The load F and displacement δ, given by the FastTrack controller, were sampled on the same time basis. The in-house developed infrared welding setup, including power electronics and pneumatics, is shown in Figure 2 (a). Figure 2 (b) shows a detail of the infrared lamps, mounted in the movable frame.

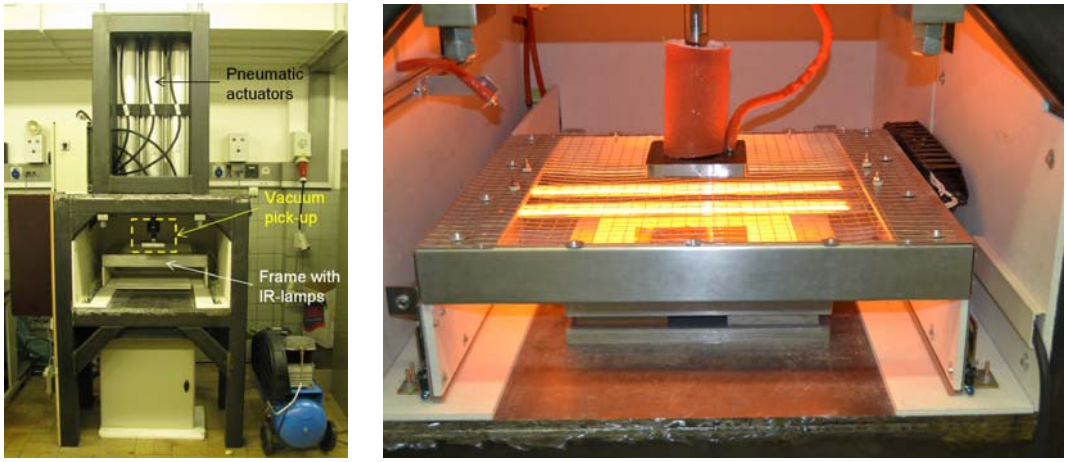

(a) Total setup *(b) IR-lights within frame*

Figure 2 – The infrared welding setup

The pneumatic actuators operate at 10 bar, yielding each a maximum force of 22.5 kN. Underneath the plunger, there is a special fixture which enables picking up a plate using vacuum. This fixture has a flat square bottom of 45 mm by 45 mm, which combined with the 22.5 kN results in a welding pressure of 1 MPa for the full area. This should be sufficient, considering the results from the hot-tool process from a previous study [11] and the fact that the original CETEX plates are hot pressed at a maximum pressure of 1 MPa. Of course, higher pressures can be achieved when smaller area's are joined together.
The infrared lights use a carbon filament and generate a power of 4000 W each. Six lamps can be mounted in the frame (Figure 2 (b) shows the two central lights) and they are controlled two by two. A separate control system continuously monitors the temperature of the specimens, using a non-contact temperature sensor or a thermocouple and controls the power sent to the IR-set.

3. Experiments and Discussion

3.1. The infrared welding process

Preliminary tests have shown that joints made between the standard specimens were of poor quality, since there was insufficient thermoplastic material present to form a joint. As such, extra layers of PPS should be added to the weld. A first attempt was made simply by laying the layers of PPS on the bottom sample and allowing them to melt in the same melting phase as the specimens. This principle, referred to as 'one sided welding' worked, but yielded poor quality and poor reproducibility of the bonds, as will be shown later. Therefore, it was decided to add the PPS in a separate phase prior to welding, as illustrated in Figure 3 (a) and (b): in a first preparation phase (Figure 3 (a), referred to as phase 1), layers of PPS are placed exactly on the location where the bond is expected (1). The remaining area of the specimen is shielded, so that this area would not melt. Next, the specimens are heated until the PPS has melted (2). In the final preparation step (3) the PPS is pushed on the surface with a polished aluminium plate, using only a mild pressure, enough to ensure a flat surface.
In the actual welding phase (Figure 3 (b), referred to as phase 2), the specimens are first placed according to the desired geometry (4). To ensure correct position of the top adherend of the lapshear specimen, a support is used. Next (5), the top specimen is lifted with the plunger and the vacuum setup and after the temperature sensor is attached to the bottom sample, both specimens are heated until the desired temperature and/or enough PPS has melted, after which the infrared lights are removed and the plunger applies the necessary consolidation pressure (6).

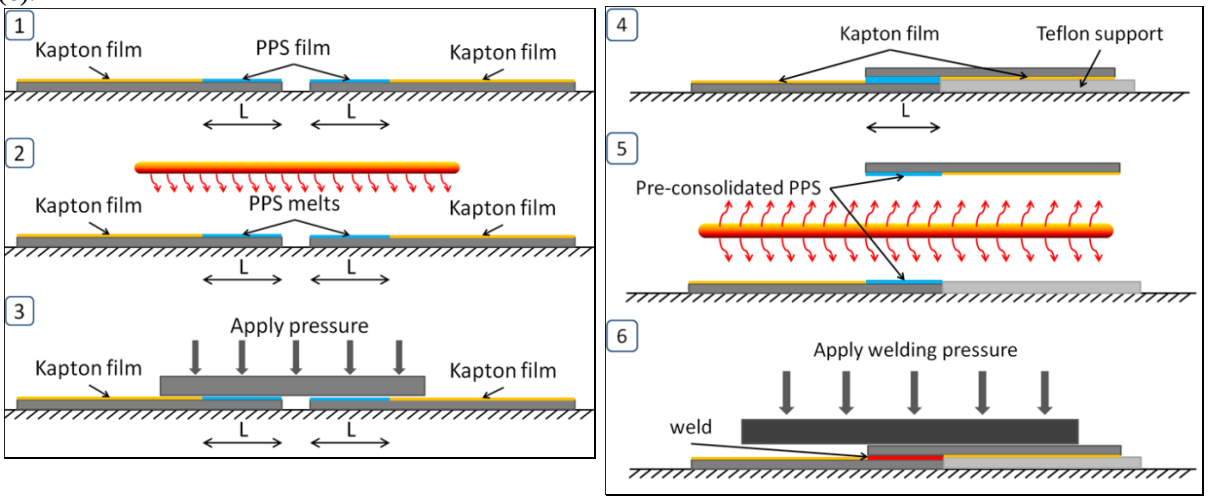

(a) Bonding PPS to the separate specimens (b) Welding the separate adherends to a specimen

Figure 3 – Welding procedure, illustrated for a lapshear specimen

The paragraph above describes the process called 'two sided welding', since PPS is pre-consolidated on both adherends prior to welding.

The next paragraph will illustrate some experiments corresponding with the optimizations of the welding parameters. These include the heating temperature and the heating time (step 5), the welding pressure and the duration (step 6). The power of the infrared lights is not taken into account, as this is already optimised in combination with the distance between the lights and the specimens, as these have a combined influence. The lower the power, the deeper the heat penetration becomes and the longer it takes before the surface melts. If the power becomes too low, then the entire specimen melts and all layers delaminate, which of course should be avoided. On the other side, the higher the power, the less deep the heat input becomes and also the shorter the melting time. However, there is a certain limit, since the PPS on the surface might burn.

The distance of the specimens to the lamps of course also has an influence. The larger the distance, the longer it takes for the specimen to melt, but the more uniform the heat on the surface becomes. After a large number of tests, an optimum was found in a distance of 55 mm between the specimen surface and the lamps, combined with 70% of power for the lamps.
After both adherends are pressed together (step 6), the cooling and consolidation time, is always taken such that the temperature of the specimen is below the softening temperature of the PPS (90°C), so that the specimen does not deform upon removal of the anvil.

4. LAPSHEAR EXPERIMENTS

As there is not yet a testing standard for fusion bonded joints, the standards regarding the testing of adhesively bonded single lap joints are considered. The geometry is chosen according to the ASTM D5868-01 '*Standard Test Method for Lap Shear Adhesion for Fiber Reinforced Plastic Bonding*'. This means that the specimen has a geometry as illustrated in Figure 1. This geometry is used for both quasi-static and fatigue testing.

4.1 Quasi-static testing for optimisation of the welding parameters

4.1.1. One sided Welding

A large number of experiments were conducted for this study, but only the most important/meaningful results are illustrated here. Table 2 shows an overview of the used parameters for the one sided welding process. The corresponding results from the lapshear experiments are shown in Figure 4, each cycle is given an offset on the horizontal axis to improve the clarity. For most welding cycles, three specimens were cut from the welded specimen. In some cases, however, only two were tested, as the third specimen was used for other quality-evaluations, not relevant for this manuscript. The consolidation time ($t_{consolidate}$), was the time to reach a temperature below 80°C, so beneath the glass transition temperature of the PPS, the column '# PPS' refers to the number of sheets of PPS (thickness 100 µm) which were added to the weld.

Table 2 – Overview of the different welding parameters for the one sided welding procedure

Welding cycle	*Pressure [MPa]*	*# PPS [-]*	t_{melt} *[s]*	$t_{consolidate}$ *[s]*
LS-8	*0.7*	*2*	*125*	*255*
LS-9	*0.7*	*2*	*130*	*250*
LS-10	*0.5*	*2*	*125*	*248*
LS-11	*0.4*	*2*	*150*	*265*
LS-16	*0.7*	*4*	*135*	*270*
LS-17	*0.7*	*0*	*120*	*265*

Cycles 8 and 9 are used as a reference, to illustrate the effect of variations in the parameters considered for the other cycles. As both have virtually the same process parameters, the reproducibility between similar welding cycles can also be assessed. As can be seen in Figure 4, the reproducibility for cycle 8 and 9 is fairly non-existent. Not only is there significant variation between specimens from both cycles, also within one cycle, the reproducibility is low. For cycles 10 and 11, the pressure during consolidation was lowered. This has a positive effect for cycle 10, resulting in higher strengths, but when the pressure becomes too low, the strength also significantly decreases. Higher pressures were also attempted, but in general, the main effect was that all liquid PPS was pushed out of the weld, resulting in poor strength. Pressures between 0.5 and 0.7 MPa seemed to be optimum values regarding this effect. For cycles 16 and 17, the amount of PPS sheets placed inside the weld was varied. For LS-16, a lot more of the liquid PPS was pushed out of the weld compared to the other cycles, partially undoing the extra layers, but nevertheless, a lower strength was achieved. More layers of PPS combined with a lower pressure, to avoid the PPS push out, also resulted in lower strengths. Using no extra sheets of PPS has an even worse effect on the failure forces of the bond, as they are the lowest of all experiments discussed here. As such, two layers of PPS seem to be an optimum for this welding procedure.

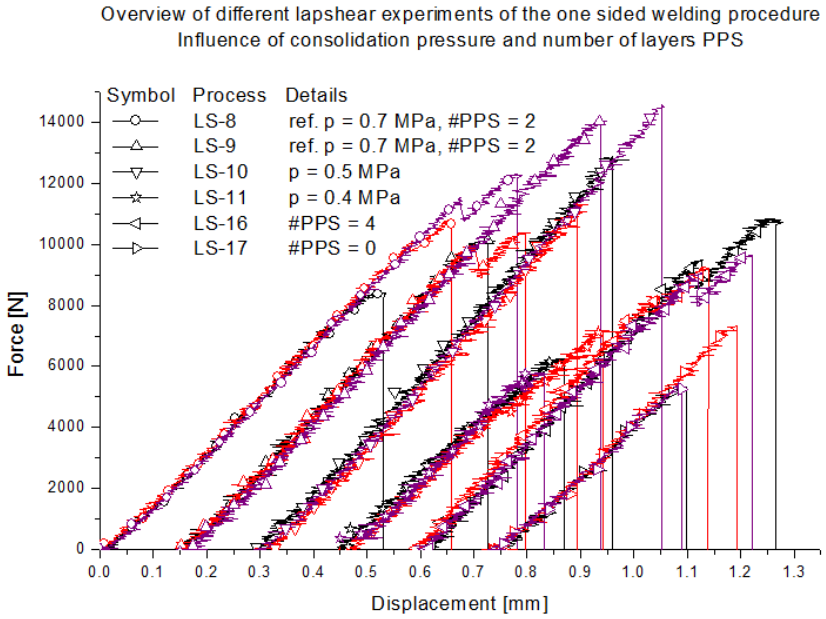

Figure 4 – Force versus displacement for the different parameter settings during the one sided welding procedure

4.1.2. Two sided welding

Table 3 gives an overview of the different sets of welding parameters considered for the two sided welding.

Table 3 – Overview of the different welding parameters for the two sided welding procedure

Welding cycle	*Pressure [MPa]*	*# PPS [-]*	t_{melt} *[s]*	$t_{consolidate}$ *[s]*
LS-22-phase1	*0.7*	*2x2*	*135*	*200*
LS-22-phase2	*0.5*		*135*	*273*
LS-23-phase1	*0.7*	*2x3*	*165*	*210*
LS-23-phase2	*0.7*		*130*	*148*
	0.5			*180*
LS-24-phase1	*0.7*	*2x1*	*135*	*225*
LS-24-phase2	*0.3*		*120*	*146*
	0.7			*260*

The corresponding results are shown in Figure 5, again with a horizontal offset between the cycles for clarity and two remarks can be made. Firstly, the reproducibility within one welding cycle is very high, especially when compared to the results from the one sided welding. Secondly, even between batches with different settings, which in some cases had a significant influence for the one sided welding procedure, the reproducibility is still remarkable. As such, a fairly large production window is present to produce qualitative results.

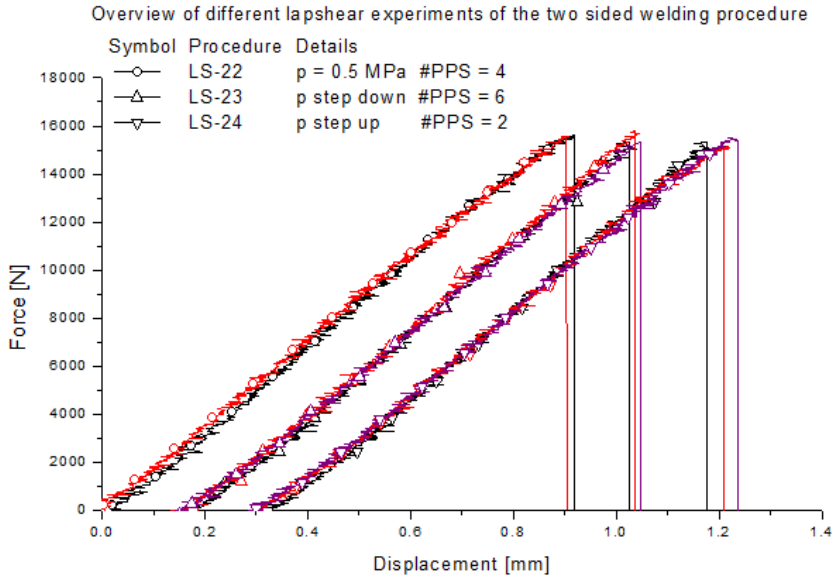

Figure 5 – Force versus displacement for the different parameter settings during the two sided welding procedure

Finally, Table 4 gives an overview of the strengths of the lapshear specimens for the different settings for both the one sided and two sided welding. For each cycle, both the average failure load ($F_{average}$) and the difference between the maximum and the minimum failure load of the tested specimens for that run is given. For comparison purposes, also the corresponding 'average shear stress' $\tau_{13}^{average}$, calculated as the failure load divided by the intended surface of 625 mm^2 and the difference between maximum and minimum are also given in the table, both in absolute value, and relative to the average value (scatter).

Table 4 – Overview of the achieved strengths for the considered welding parameters

Welding Cycle	$F_{average}$ *[N]*	$F^{max} - F^{min}$ *[N]*	$\tau_{13}^{average}$ *[MPa]*	$\tau_{13}^{max} - \tau_{13}^{min}$ *[MPa]*	*scatter [%]*
		One sided welding			
LS-8	*10363*	*3918*	*16.58*	*6.27*	*38*
LS-9	*11512*	*3934*	*18.42*	*6.29*	*34*
LS-10	*12922*	*3254*	*20.67*	*5.21*	*25*
LS-11	*6380*	*1383*	*10.21*	*2.21*	*22*
LS-16	*9900*	*1590*	*15.84*	*2.54*	*16*
LS-17	*3901*	*1306*	*6.24*	*2.09*	*33*
		Two sided welding			
LS-22	*15589*	*29*	*24.94*	*0.05*	*0.2*
LS-23	*15485*	*432*	*24.78*	*0.69*	*2.8*
LS-24	*15288*	*289*	*24.46*	*0.46*	*1.9*

Although the one sided welding sometimes yields high failure loads, the scatter on these results is very high, making this procedure unpredictable. As such, the two sided welding is preferable, as the achieved strength is not only higher, it is also combined with very low scatter, making it more predictable.

4.2. Fatigue testing

Given the very promising results of the two sided welding procedure and the rather poor reproducibility of the one-sided process, only the two sided welding was considered for the fatigue loading conditions. All fatigue experiments were performed in load-control between 0.5 kN, to avoid possible buckling due to overshoot of the machine and the corresponding compressive load, and a certain maximum load, related to the failure strength; all tests were performed at 2Hz, to avoid possible heating and corresponding thermal deterioration of the weld. During a fatigue test, every five minutes, five cycles are registered by the DAQ-system in order to obtain an overview of what is happening during the test.

Of course, a clear relation between the maximum load and fatigue life is visible. For a test at 75% of the average failure load, the specimen failed quite sudden after only 1350 cycles. During this test, there was no significant change in specimen stiffness visible, nor permanent deformation.

For a second load range, a specimen was tested at 60% of the failure load and this specimen failed after 13165 cycles. During this test, little permanent deformation was present and also a little stiffness degradation, but

again, the failure seemed quite brittle. Therefore, a third load level was tested, namely at 45% of the failure load. The evolution of the maximum, minimum and mean value of the displacement during the test is illustrated in Figure 6. Given the fact that it is a load-controlled test, an increase in difference between the maximum and minimum value of the displacement suggests a stiffness reduction, whereas an increase in minimum value of the displacement suggests permanent deformation. It can be noted that near the end of fatigue life, there is a steady increase in all displacement values, suggesting an increase in crack growth.

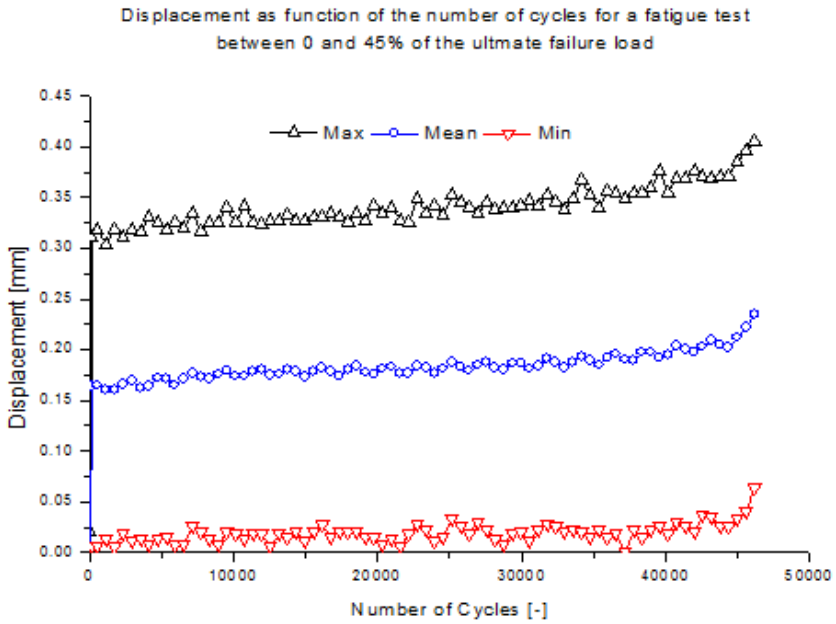

Figure 6 – Fatigue experiment between 0 and 45% of the failure load

Figure 7 illustrates the hysteresis loops of selected measurements throughout the fatigue life. The cycle number represents the first cycle of the five being measured. Also here, the increase in permanent deformation and the decrease in specimen stiffness can be seen. It should be noted that especially near the end of life (cycle 46768 was the last measured before failure of the specimen), these phenomena become more apparent, as could also be derived from Figure 6.

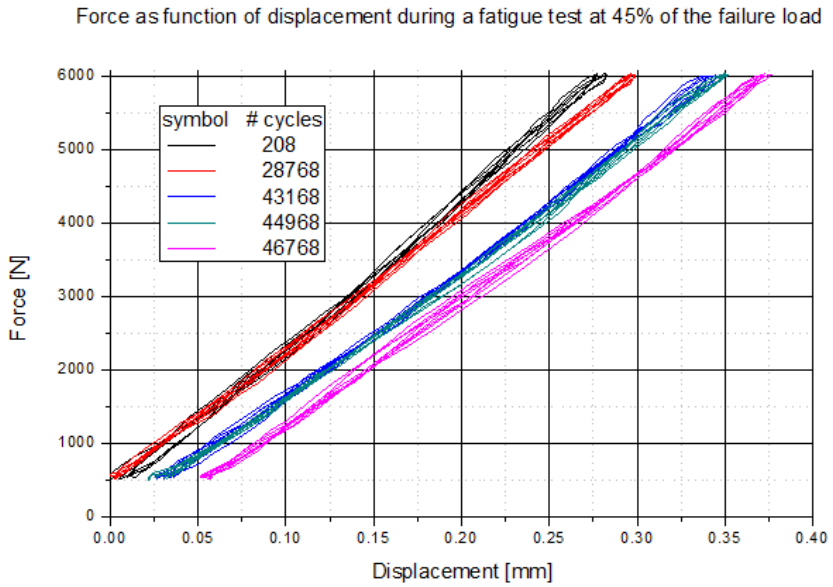

Figure 7 – Hysteresisloops during the fatigue test at various times in fatigue life

To observe the crack growth, a specimen was polished before a similar fatigue test was conducted and the test was paused regularly to perform a quasi-static test with a microscope mounted in front of the specimen. The reason for performing a test rather the just observing the specimen under a microscope is that all cracks are opened due to the loading. By keeping the static load under the maximum load of the fatigue test, it is ensured

that no extra damage is imposed during these tests. It should be noted that the quasi-static test revealed no extra information with respect to the hysteresis loops during the fatigue test as depicted in Figure 7.
Figure 8 illustrates the crack early in fatigue life, once for a static test done after 10 000 cycles and once for a static test after 20 000 cycles. The top image shows the polished side of the overlap at 0.5 kN loading after 10 000 cycles, and as can be seen, it is very hard to distinguish any cracks. By applying 5.5 kN load (middle pictures), the crack can be distinguished as it opens due to the bending moment, inherent to the lapshear specimen. The bottom picture illustrates the loaded specimen after 20 000 cycles and the crack has grown over about halve of a weft yarn.
Unfortunately, due to a power problem, the machine powered down and the specimen failed as a consequence prior to reaching 30 000 cycles, so no other pictures are present of this specimen.

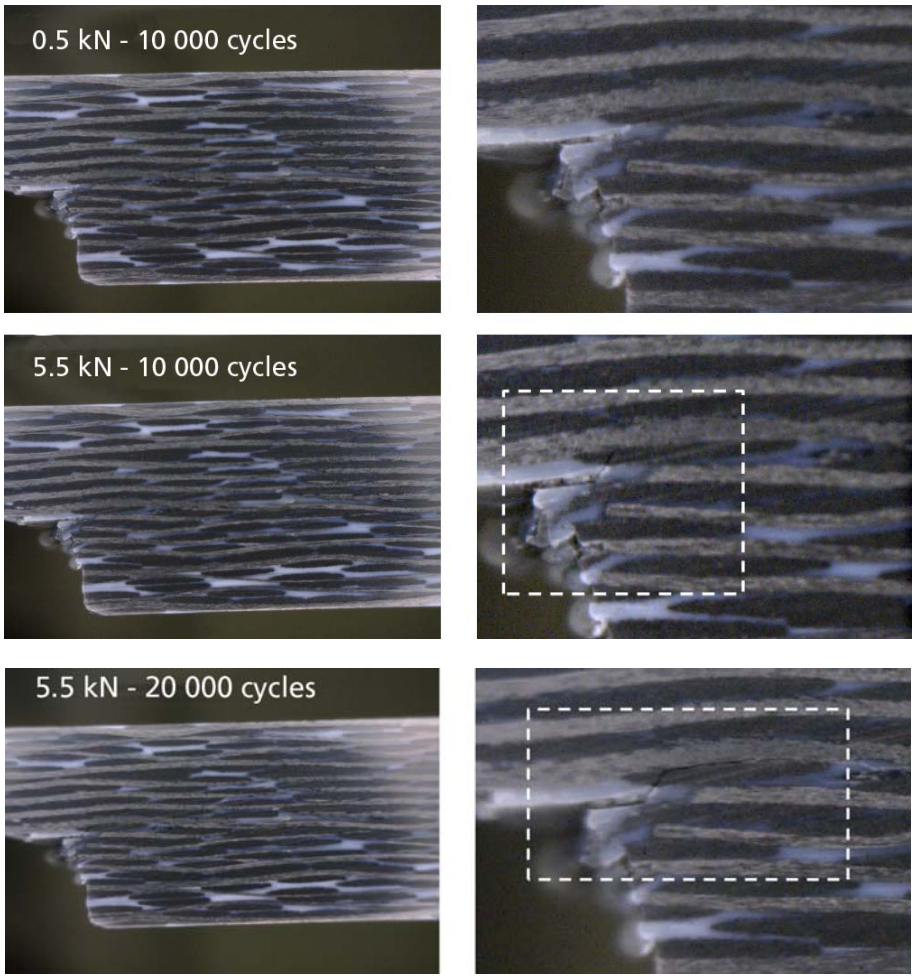

Figure 8 – Illustration of the crack growth during a fatigue test at 45% of the failure load

When visualising the failure area of a test specimen, loaded in fatigue at 45% of the failure load, two different failure regions can clearly be distinguished. Figure 9 illustrates the overlap area of the lapshear specimen from which the fatigue results were depicted in Figure 6. The crack starts to grow from the outside of the overlap and grows gradually at both sides with each cycle, until the remaining area (within the rectangle in Figure 9) is too small to carry the entire load, causing failure. As can be seen, significant crack growth is present under these loading conditions, explaining the decrease in stiffness and the increase in permanent deformation. It should be noted that such extensive crack growth does not occur for static failure, the crack starts to grow, but the minimum area required to carry the load is reached a lot earlier.

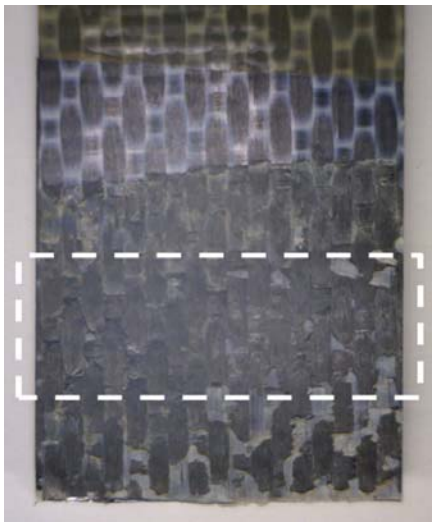

Figure 9 – Illustration of the failed overlap region of a fatigue specimen tested at 45% failure load.

5. CONCLUSIONS

This manuscript studied the infrared welding process for a 5-harness satin weave carbon reinforced polyphenylene sulphide. The quality and strength of the welded joints were assessed using lapshear experiments according to the ASTM D5868-01 '*Standard Test Method for Lap Shear Adhesion for Fiber Reinforced Plastic Bonding*', as there is not yet a standard for fusion bonded joints. Two types of welding procedures were assessed, where the main difference lies in the way extra sheets of PPS are added to the bond. For the so-called one sided welding, the PPS was put on the bottom specimen and was melted during the heating phase of the process, meaning it melted together with the surfaces of top and bottom specimen. For the so-called two sided welding, the layers of PPS were added in an extra phase, prior to the welding. The same amount of layers was added on both specimens, for symmetry purposes, after which they were melted and consolidated under pressure.

It was found that although high failure loads were possible, the one sided welding yielded very irreproducible results, not only between separate welding cycles with the same settings, but also between the three specimens coming from one cycle, which of course cannot be allowed.

The two sided welding showed very reproducible results, both within one welding cycle as when comparing different welding cycles. Furthermore, there seems to be little influence, within certain boundaries, of the amount of PPS added and the consolidation pressure, yielding a bigger process window.

With respect to the fatigue behaviour, there is a significant influence of the maximum load level on the fatigue life. Crack growth occurs already form the first cycles on and when lower load levels are considered, a significant amount of crack growth occurs before final failure, as was visualised both by observing the overlap region of a failed specimen and by doing microscopic observations of the polished side of a specimen during the fatigue test.

ACKNOWLEDGEMENTS

The authors are highly indebted to the Fund of Scientific Research – Flanders (F.W.O.) for sponsoring this research and to Ten Cate Advanced Composites for supplying the material. Also special thanks to L. Vanden Broecke for his contributions to this work.

REFERENCES

1. Yousefpour A, Hojjati M, Immarigeon JP. *Fusion bonding/welding of thermoplastic composites*. Journal of Thermoplastic Composite Materials, 2004, (17 (4), pp 303-341).
2. Bhaskar Patham and Peter H. Foss. *Thermoplastic Vibration Welding: Review of Process Phenomenology and Processing–Structure–Property Interrelationships*. Polymer Engineering Science, 2011, (51 pp 1–22).
3. Fernandez V.I. and Bersee, H.E.N. *Ultrasonic Welding of Advanced Thermoplastic Composites: An Investigation on Energy-Directing Surfaces*. Advances in Polymer Technology, 2010, (29 (2), pp 112–121).
4. Ageorges C, Ye L. *Resistance welding of thermosetting composite/thermoplastic composite joints*. Composites Part A-Applied Science and Manufacturing, 2001, (32 (11), pp 1603-1612).
5. Stavrov D, Bersee HEN. *Resistance welding of thermoplastic composites - an overview*. Composites Part A-Applied Science and Manufacturing, 2005, (36 (1), pp 39-54).
6. Kagan VA, Nichols RJ. *Benefits of induction welding of reinforced thermoplastics in high performance applications.* Journal of Reinforced Plastics and Composites, 2005, (24 (13), pp 1345-1352).
7. W. Suwanwatana, S. Yarlagadda and J.W. Gillespie, Jr. *Hysteresis heating based induction bonding of thermoplastic composites*. Composite Science and Technology, 2006, (66 (11-12),pp 1713-1723).
8. Lamethe JF, Beauchene P, Leger L. *Polymer dynamics applied to PEEK matrix composite welding*. Aerospace Science and Technology, 2005, (9 (3), pp 233-240).
9. Szekrenyes, Andras. *Improved analysis of unidirectional composite delamination specimens.* Mechanics of Materials, 2007, (39 (10) pp 953-974).
10. Mathews, Mary J. and Swanson, Stephen R. *Characterization of the interlaminar fracture toughness of a laminated carbon/epoxy composite*. Composite Science and Technology, 2007, (67 (7-8) pp 1489-1498).
11. De Baere I., Van Paepegem W. and Degrieck J. *Feasibility study of fusion bonding for carbon fabric reinforced polyphenylene sulphide by hot-tool welding*. Journal of Thermoplastic Composite Materials, 2012 (25 (2) pp 135-151)